



HAL
open science

Considering waning immunity to better explain dengue dynamics

Leonardo López, Richard E. Paul, Van-Mai Cao-Lormeau, Xavier Rodó

► **To cite this version:**

Leonardo López, Richard E. Paul, Van-Mai Cao-Lormeau, Xavier Rodó. Considering waning immunity to better explain dengue dynamics. *Epidemics*, 2022, 41, pp.100630. 10.1016/j.epidem.2022.100630 . pasteur-04009098

HAL Id: pasteur-04009098

<https://pasteur.hal.science/pasteur-04009098v1>

Submitted on 1 Mar 2023

HAL is a multi-disciplinary open access archive for the deposit and dissemination of scientific research documents, whether they are published or not. The documents may come from teaching and research institutions in France or abroad, or from public or private research centers.

L'archive ouverte pluridisciplinaire **HAL**, est destinée au dépôt et à la diffusion de documents scientifiques de niveau recherche, publiés ou non, émanant des établissements d'enseignement et de recherche français ou étrangers, des laboratoires publics ou privés.



Distributed under a Creative Commons Attribution - NonCommercial - NoDerivatives 4.0 International License



Considering waning immunity to better explain dengue dynamics

Leonardo López^{a,*}, Richard E. Paul^b, Van-Mai Cao-Lormeau^c, Xavier Rodó^{a,d,*}

^a CLIMA (Climate and Health) Program, ISGlobal, c/Dr. Aiguader 88, 08003 Barcelona, Spain

^b Institut Pasteur, Université de Paris, CNRS UMR2000, Ecology and Emergence of Arthropod-borne Pathogens Unit, F-75015 Paris, France

^c Laboratoire de recherche sur les maladies infectieuses à transmission vectorielle, Institut Louis Malardé, 98713 Papeete, Tahiti, French Polynesia

^d ICREA, Passeig de Lluís Companys 23, 08010 Barcelona, Spain

ARTICLE INFO

Dataset link: <https://figshare.com/s/deebd75b84e742c1803f>

Keywords:

DENV
Dengue
French
Polynesia
Monotypic
Epidemics
Immunity
Vaccine
Model

ABSTRACT

Life-long serotype-specific immunity following dengue virus infection may not always occur, but the true extent of this effect is unknown. Analysis of more than 20 years of monotypic epidemics in the isolated French Polynesian islands revealed that whilst the risk of symptomatic dengue infection did conform to the classical paradigms of homotypic immunity and increased disease risk in heterotypic secondary infections, incorporation of waning immunity improved the ability of epidemiological models to capture the observed epidemic dynamics. Not only does this show how inclusion of waning immunity into classical models can reveal important facets of the immune response to natural dengue virus infection, it also has significant ramifications for vaccine development and implementation in dengue endemic areas.

1. Author summary

Waning immunity drives dengue epidemics and will undermine vaccine efficacy.

2. Introduction

Dengue poses an increasing public health burden and is caused by any one of four viral serotypes (DENV-1,-2,-3,-4). Lifelong serotype specific immunity and cross-reactive disease enhancing immunity (antibody dependent enhancement) are paradigms for dengue (Halstead et al., 2003). Recent serological studies have, however, suggested that these paradigms might not be entirely true (Katzelnick et al., 2017; Gallichotte et al., 2018). Not only are dengue virus serotypes not so immunologically segregated as thought, but also sterilising serotype-specific immunity may not always follow infection (Katzelnick et al., 2015). Re-susceptibility of individuals with a homotypic serotype has been previously described (Endy et al., 2004; Waggoner et al., 2016) and dengue infections in individuals with non-dengue like symptoms develop much poorer immune responses (Waggoner et al., 2017). It remains unknown what long term immune consequences follow on from the broadly different regulation of immune genes in asymptomatic infections (Yeo et al., 2014). Population-wide empirical data on the

epidemiological consequences of these uncertain immunological responses are, however, lacking. This is largely due to the confounding effects of co-circulation of different serotypes in most endemic settings, the inability of serology to categorise either the number or the order of serotype infections and the large but variable proportion of unreported, asymptomatic infections (Salje et al., 2014; Grange et al., 2014). Resolving this uncertainty is crucial for predicting disease risk and for vaccine development, as recently highlighted by the abortive Dengvaxia vaccine in the Philippines (Halstead et al., 2020).

In contrast to other endemic settings, French Polynesia, an isolated group of islands in the South Pacific (Fig. 1), has recorded 15 mono serotype dengue epidemics of all four serotypes since 1944, and offers a simpler but also unique epidemiological setting to examine the immuno-epidemiology of dengue (Aubry and Cao-Lormeau, 2019). From our 35-year database of laboratory-confirmed geolocated cases with age and gender (1979–2014), seven monotypic and one multitypic epidemic occurred, followed for the most part by long periods of low-level inter-epidemic transmission (Teissier et al., 2020)(Fig. 1). Through analysis of consecutive epidemics over this 35-year period and implementation of novel dynamical models, this work assesses the evidence supporting the classical dengue paradigms, evaluates the epidemiological importance of asymptomatic infections and addresses the role of waning homotypic immunity.

* Corresponding authors.

E-mail addresses: leonardorafael.lopez@isglobal.org (L. López), xavier.rodó@isglobal.org (X. Rodó).

<https://doi.org/10.1016/j.epidem.2022.100630>

Received 17 November 2021; Received in revised form 25 July 2022; Accepted 20 September 2022

Available online 10 October 2022

1755-4365/© 2022 The Author(s). Published by Elsevier B.V. This is an open access article under the CC BY-NC-ND license (<http://creativecommons.org/licenses/by-nc-nd/4.0/>).

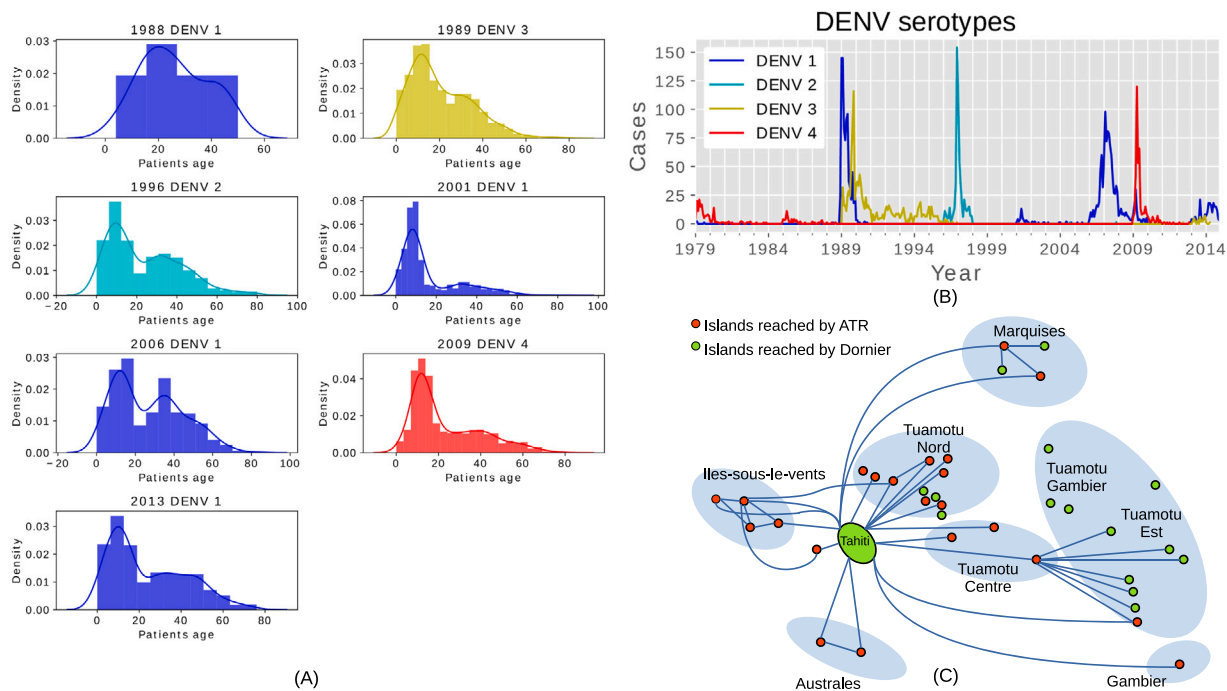


Fig. 1. The age distribution, time series of DENV strains, and island connections .(A) Density plot of the age distribution for the main DENV strains in French Polynesia. Most of the cases are under 20 years old. The DENV-1 epidemics waves are plotted in blue, DENV-2 is plotted in cyan, DENV-3 is plotted in yellow and DENV-4 is plotted in red to make the age distributions (B) 1979–2014 time series of the main DENV serotype in French Polynesia. The colour scheme of the time series follows the same scheme as the age distributions (C) Graph diagram showing the main connections between islands and archipelagos. In this graph red and green dots represents islands, those islands in the same cluster are inside the blue shaded areas. Connections between clusters and islands are plotted as blue lines. (For interpretation of the references to colour in this figure legend, the reader is referred to the web version of this article.)

The manuscript is organised as follows: In Section 3 we give a detailed explanation of the different statistical and numerical methods we use to analyse the data. Within this section, the data used and their sources are described in Sections 3.1 and 3.2. Section 3.3 provides a detailed explanation of the statistical analyses performed on the data; the results obtained from these analyses justify the work carried out with the mechanistic model introduced in Section 3.4. This model was fitted with the data described in Section 3.2, this process is documented in Sections 3.5 and 3.6. The results obtained from all these analyses and simulations are duly presented in Section 4 and discussed in Section 5.

3. Methods

3.1. Study site and population

As previously described (Teissier et al., 2020), French Polynesia is located in the middle of the Pacific Ocean and is composed of 117 islands (ISPF, 2018), grouped into five administrative subdivisions: the Windward Islands (five islands), the Leeward Islands (nine), the Marquesas Islands (Descloux et al., 2009), the Austral Islands (seven) and the Tuamotu-Gambier Islands (68 and 16, respectively). Out of the 72 inhabited islands, only 15 have a population greater than 1000 individuals, four (Moorea, Raiatea, Bora-Bora and Tahiti) have more than 10,000 and only Tahiti numbers over 100,000; at the last 2017 census, 68.7% of the total population of 275,918 lived on Tahiti (ISPF, 2018). Island population sizes and age distributions of French Polynesia used in this study were taken from the past censuses (1971, 1983, 1988, 1996, 2002, 2007 and 2012) to cover the period of time seen in the dengue analysis database (ISPF, 2018). Fig. 1-C summarises the topological structure of the different archipelagos that make up the scenario. The main air connections between islands of the same archipelago and different archipelagos are summarised. As can be seen, Tahiti is the central node of the network.

3.2. Dengue case data

French Polynesia has succumbed to epidemics of all four serotypes since 1944: DENV-1 (1944, 1975, 1988, 2001, 2006, 2013), DENV-2 (1972, 1996), DENV-3 (1964, 1989), DENV-4 (1979, 2009). The Institut Louis Malardé, Tahiti, has recorded dengue suspected and confirmed cases from March 1975 with records of age and location since 1979. Confirmation of cases used Haemagglutination Inhibition assay (1975–1988), ELISA (IgM)(1986–2003), isolation of DENV on mosquito C6/36 cell cultures (1984–2005) or RT-PCR (from 2000). The data are fully available and can be accessed via this link <https://figshare.com/s/deebd75b84e742c1803f>.

3.3. Statistical analyses

The extent of impact of homotypic or heterotypic immunity on incidence rates (per sub-division) was assessed through age-stratification of cases according to having been born (or not) prior to the previous epidemic periods of (a) a previous epidemic of the same serotype; (b) a previous epidemic of any serotype. Statistical analyses were performed, fitting age group stratified by previous exposure and the archipelago-specific attack rate as explanatory variables in a loglinear regression of number of cases with log transformed population size fitted as an offset. For the homotypic analyses, heterotypic exposures were ignored. For heterotypic analyses, the age stratification only considered the first exposure to a specific heterotypic serotype but all previous homotypic exposures. Demographic data are aggregated into the following age groups: 0–1y, 1–4y, 5–9y, 10–14y, 15–19y, 20–29y, 30–39y, 40–49y, 50–59y, 60–69y, 70–79y, 80+y. This therefore places some limitation on the age stratification possible.

Thus, for analysis of the 1988 DENV-1 epidemic, the age group stratification for heterotypic exposure were: < 10 years old (the unexposed reference population), 10–19 years(exposed to the DENV-4 1979 epidemic), 20–29 (exposed to the DENV-2 1972 epidemic) and

30+ years (exposed to the DENV-3 1964 epidemic). The homotypic age stratification fell into 3 groups < 15y for no previous exposure, 15–49y for the 1975 DENV-1 epidemic and > 50y for the DENV-1 1944 epidemic.

For the 1989 DENV-3, because it occurred immediately after the 1988 DENV-1 epidemic, this exposure was ignored (because of zero ages unexposed). Heterotypic exposure age stratification was thus: < 10y (unexposed reference group), 10–14y (exposed to DENV-4 1979 epidemic), 15–19y (DENV-1 1975 epidemic), 20+ (exposed to the DENV-2 1972 epidemic) and 30+ for homotypic exposure during the DENV-3 (1964 epidemic).

For the DENV-2 1996 epidemic, heterotypic exposure age stratification was: < 5y (zero exposure, reference group), 5–9y (exposure to the 1989/90 DENV-3 epidemic), 10–14y (exposure to the 1988 DENV-1 epidemic), 15–19y (exposure to the 1979 DENV-4 epidemic) and 20 + y previous homotypic exposure (DENV-2 1972 epidemic).

For the DENV-1 2001 epidemic, heterotypic exposure age stratification was: < 5y (zero exposure, reference group), 5–9y (exposure to the 1996 DENV-2 epidemic), 10–19y (exposure to the 1989 DENV-3 epidemic), 20 + y (exposure to the 1979 DENV-4 epidemic). Homotypic age stratification was: < 15y zero, 15–29y first exposure (1988 epidemic), 30–69y two exposures (1975 epidemic) and 70 + y three exposures (1944 epidemic).

For the DENV-1 2006 epidemic, heterotypic exposure age stratification was: < 10y zero exposure (reference group), 10–14y (exposure to the 1996 DENV-2 epidemic), 15–29y (exposure to the 1989 DENV-3 epidemic), 30 + y (exposure to the 1979 DENV-4 epidemic). Homotypic age stratification was: < 5y zero, 5–19y first exposure (2001 epidemic), 20–29y two exposures (1988 epidemic), 30–69y three exposures (1975 epidemic) and 70 + y four exposures (1944 epidemic).

For the DENV-4 2009 epidemic, heterotypic exposure age stratification was: < 5y (zero exposure, reference group), 5–14y (exposure to 2001/2006 DENV-1 epidemics), 15–24y (exposure to the 1996 DENV-2 epidemic) (here the 20–29 demographic class was divided by two), 25 + y (exposure to the 1989 DENV-3 epidemic). Homotypic ages stratification were < 30y, and > 30y (exposure or not to 1979 DENV-4 epidemic).

All analyses were performed in Genstat vers 15 (Payne, 2009) and results shown are significant at $P < 0.05$.

3.4. Model

The proposed model is a simple strain population-based model that follows a *SIRS* dynamic. The dynamics of the model are described in Fig. 3. For the age structured model, we divide the population into two age groups, reflecting the age-incidence distribution shown in Fig. 1-A, namely *Y* (young, ≤ 20 years old) and *A* (adults, > 20 years old). The parameter ϵ defines the rate at which individuals move from the young to the adult age category. After an incubation time τ_1 post-exposure, a proportion P_h of individuals move to the symptomatic infected population (I_i) and a proportion $1 - P_h$ of the individuals moves to the infected asymptomatic population (A_i) at rate β_i . Finally, after a recovery period τ_2 , symptomatic and asymptomatic populations move to the recovered state (R_i), where $i = Y, A$. The parameter δ_{si} (with $i = Y, A$ for age structured model) represents the re-susceptibility rate of the recovered population, to evaluate the effect of immunity loss. The dynamics of this model are governed by Eqs. (1) and (2):

The infection force β was decomposed in two terms, one seasonal (*S*) and another inter-annual (*IA*) as shown in Fig. 3. On the other hand, the δ parameter was added to this parameter as a scalar factor to adequately reproduce the outbreak dynamics in terms of amplitude. We divide the infection force into two components to identify fluctuations in transmission rates that seasonality alone cannot explain. In particular, this formulation allows incorporating mechanisms that influence the inter-annual variability in the infection force rate as the result of a modulation of the seasonality in transmission rates. In other words, this decomposition in the infection force is very relevant when the series shows significant interannual variability over constant seasonal

changes This way, we set initial values according to the previous waves so we are properly considering the effect of seasonal infection force. This formulation also helps improve the fitting without over-penalisation for the addition of an extra compartment in the model and it can give an idea of whether there are different factors contributing to the seasonality and to year-to-year changes. These seasonal and inter-annual terms in the forces of infection are determined by the ω_i (with $i = S, IA$) parameters, which determines these two different time periods for the cosine function. The μ parameter was not adjusted and its value was established from the aforementioned census data. On the other hand, according to Eqs. (1) and (2), it can be seen that the population is assumed to be constant since the action of μ is compensated as inputs and outputs proportional to the size of the population For simplicity, we assume the same recovery (γ) rate for both symptomatic and asymptomatic populations. The influence of the asymptomatic population can be tracked by the P_h parameter.

$$\begin{aligned} \dot{S} &= \mu (N_h - S) + \delta_* R - \beta S/N_h, \\ \dot{I} &= P_h \beta \tau_1 S/N_h - (\mu + \gamma) I, \\ \dot{A} &= (1 - P_h) \beta \tau_1 S/N_h - (\mu + \gamma) A, \\ \dot{R} &= \gamma (I + A) \tau_2 - \mu R - \delta_* R, \\ \dot{S}_Y &= \mu (N_h - S_Y) + \delta_{Y*} R_Y - \beta_Y S_Y/N_h - \epsilon S_Y, \\ \dot{I}_Y &= P_h \beta_Y \tau_1 S_Y/N_h - (\mu + \gamma_Y) I_Y - \epsilon I_Y, \\ \dot{A}_Y &= (1 - P_h) \beta_Y \tau_1 S_Y/N_h - (\mu + \gamma_Y) A_Y - \epsilon A_Y, \\ \dot{R}_Y &= \gamma_Y (I_Y + A_Y) \tau_2 - \mu R_Y - \epsilon R_Y - \delta_{Y*} R_Y, \\ \dot{S}_A &= \mu (N_h - S_A) + \delta_{A*} R_A - \beta_A S_A/N_h + \epsilon S_Y, \\ \dot{I}_A &= P_h \beta_A \tau_1 S_A/N_h - (\mu + \gamma_A) I_A + \epsilon I_Y, \\ \dot{A}_A &= (1 - P_h) \beta_A \tau_1 S_A/N_h - (\mu + \gamma_A) A_A + \epsilon A_Y, \\ \dot{R}_A &= \gamma_A (I_A + A_A) \tau_2 - \mu R_A + \epsilon R_Y - \delta_{A*} R_A. \end{aligned} \tag{1}$$

$$\tag{2}$$

The one population and two population models are summarised in Fig. 3. In this figure it can be observed that the seasonal and inter-annual terms are multiplied to calculate the global force of infection. This is because we assume independence between the two terms

3.5. Model fitting

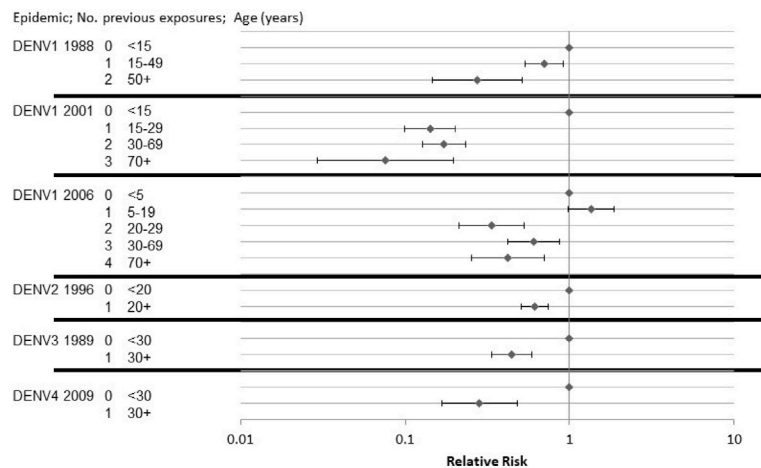
Model fitting was performed through a nonlinear programming optimisation method to find the minimum estimate of a constrained nonlinear function. The minimised function is the Normalised Square Error (*NSE*) as shown in Eq. (3). It is necessary to understand that the equation below is a measure of the error associated with the minimised parameters. We chose this function because it is an easy to calculate evaluation metric, all the errors are weighted on the same scale since absolute values are taken and it provides an even measure of how well the model is performing.

$$NSE = \sqrt{\sum_{i=1}^N \left(\frac{I_i^{model} - I_i^{observed}}{\sum_{i=1}^N I_i^{observed}} \right)^2}, \tag{3}$$

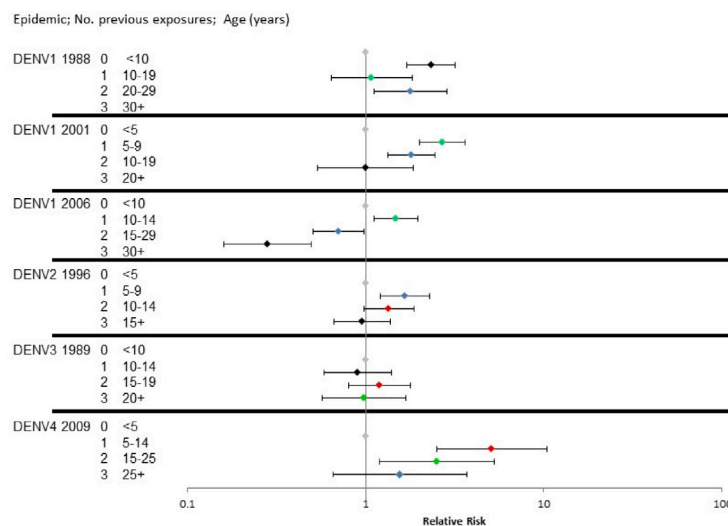
where I_i^{model} is the infected symptomatic population predicted for the model and $I_i^{observed}$ is the observed infected symptomatic population and N is the number of samples. The Sequential quadratic programming (*SQP*) algorithm is an iterative method for constrained nonlinear optimisation. Solving a sequence of optimisation sub-problems, each of which optimises a quadratic model of the objective subject to a linearisation of the constraints, the objective function $f(x)$ is minimised. The optimisation problem takes then the following configuration

$$\begin{aligned} \min_x & f(x) \\ \text{s.t} & lb \geq x \geq ub, \end{aligned} \tag{4}$$

where $f(x)$ is Eq. (3) and, x is a vector containing the parameters to be minimised, $lb = 0$ is the lower bound and $ub = 1$ is the upper bound.



(A)



(B)

Fig. 2. Relative Risk of incidence rates of confirmed dengue cases stratified by age group. Respect to (A) Potential previous exposure to the same serotype during previous epidemics. (B) Potential previous exposure to any serotype during previous epidemics. No previous exposure age group used as the reference group and denoted as 0. Horizontal axis denotes the relative risk of infection, the vertical axis denotes the number of previous exposures to the same or different serotypes.

The age group stratification for heterotypic exposure were for 1988 DENV-1: < 10y, 10–19y, 20–29y and > 30y; for 1989 DENV-3: < 10y, 10–14y, 15–19y and > 20y; for DENV-2 1996: < 5y, 5–9y, 10–14y and 15–19y; for DENV-1 2001: < 5y, 5–9y, 10–19y and > 20y; for DENV-1 2006: < 10y, 10–14y, 15–29y and > 30y; for DENV-4 2009: < 5y, 5–14y, 15–24y, 20–29y and > 29y.

The homotypic age stratification were for 1988 DENV-1: < 15y, 15–49y and > 50y; for 1989 DENV-3 > 30y; for DENV-2 1996: > 20y; for DENV-1 2001: < 15y, 15–29y, 30–69y and > 70y; for DENV-1 2006: < 5y, 5–19y, 20–29y, 30–69y and > 70y; for DENV-4 2009: < 30y and > 30y.

For the model with two population classes, we fit 8 parameters and $x = \{\beta_{SY}, \beta_{LAY}, \gamma_Y, \delta_{Y*}, \beta_{SA}, \beta_{LAA}, \gamma_A, \delta_{A*}\}$; $lb = \{0, 0, 0, 0, 0, 0, 0, 0\}$ and $ub = \{1, 1, 1, 1, 1, 1, 1, 1\}$. For the single population model, we fit 4 parameters and then $x = \{\beta_S, \beta_{LA}, \gamma, \delta_*\}$; $lb = \{0, 0, 0, 0\}$ and $ub = \{1, 1, 1, 1\}$. We used MATLAB to both run the models and simulate the adjustments. The fitting was run using the *fmincon* function with the ‘active-set’ algorithm. The maximum number of iterations used was 1000 iterations, the maximum number of evaluations for the objective function (Eq. (3)) was 1000 evaluations and the established error tolerance was $1e - 14$. Finally, 500 iterations were run to have the fit achieve a representative parameter space. The parameters obtained are shown in Table 1, for the model of one population and in Table 2 for the model of two populations.

Simulations in the optimisation process begin on the dates shown in the dataset plots. This means when the start of the outbreak is reported and the first disease cases are observed. The initial conditions for both models were fixed to normalise the populations of the compartments

with the total population size N_h . The N_h value was 200000 for the 1989 DENV-3 wave, 215000 for the 1996 DENV-2 wave, 245000 for the 2001 DENV-1 wave and 260000 for the 2006 DENV-1 wave. For the two population model the N_h was divided between sub-20 years (45%) and over-20 years (55%). The initial infected population was fixed with values near to 0 since the infections mostly depend on the force of infection, which implicitly incorporates the infection by mosquitoes bites, more specifically the $I(0) \in [0, 1e - 5]$; the same assumption was made for both models (one and two populations). To incorporate the influence of previous infections of a particular DENV strain, the $R(0)$ population was fixed taking into account the number of previous infections taken from the reported data (see Data and materials availability), we set the recovered population using this criterion because of simplicity in the model and because of the lack of information regarding the distribution of times individuals might have spent in that specific compartment and the period since prior infection. Doing this we ensure to fix the initial conditions of the models to the real system conditions. In all the cases, the initial populations were normalised using the N_h factor.

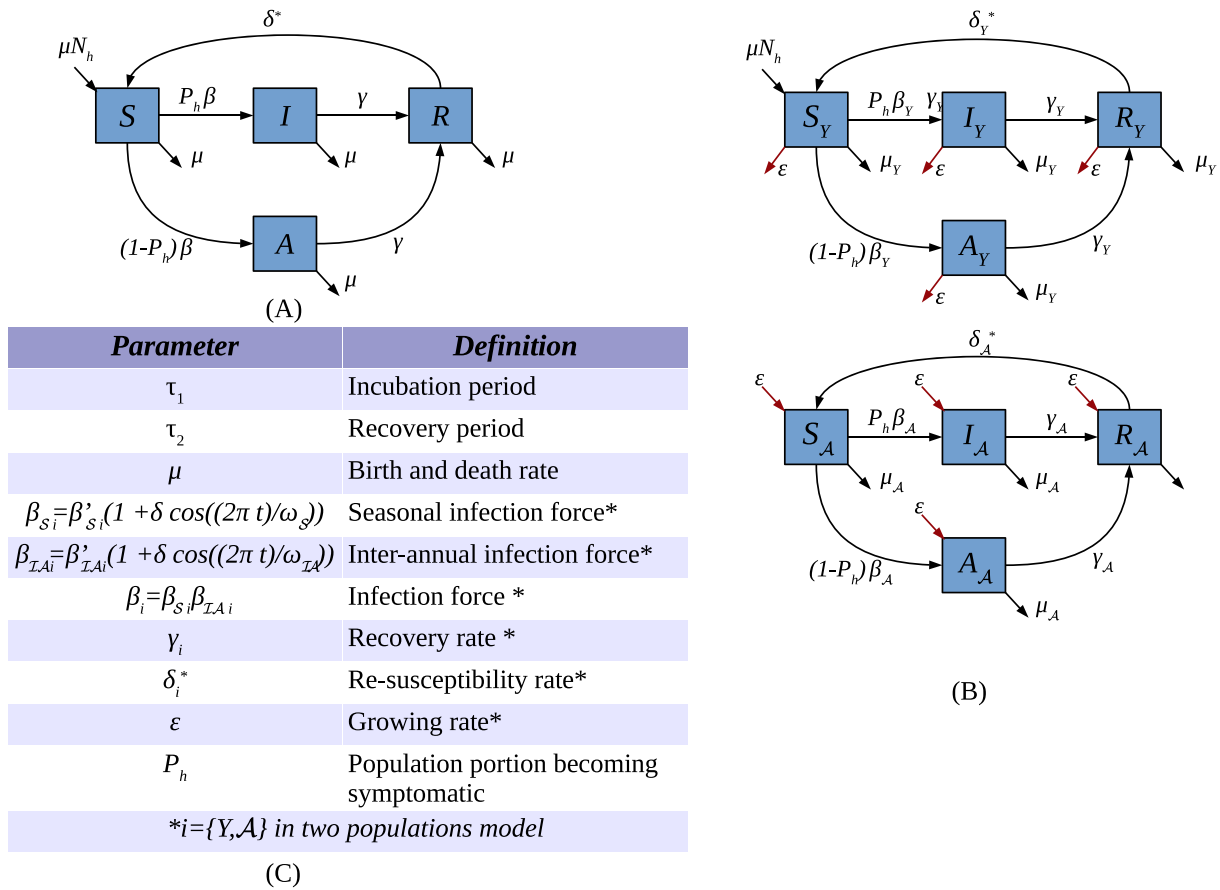


Fig. 3. Model configurations used in this study. (A) Block diagram of the single population model; S (susceptible); I (Infectious); A (Asymptomatic) and R (Recovered). (B) Block diagram of the model of two populations; S_Y (Young susceptible); I_Y (Young infectious); A_Y (Young Asymptomatic) and R_Y (Young Recovered); S_A (Susceptible adults); I_A (Infectious Adults); A_A (Asymptomatic adults) and R_A (Recovered adults). (C) Model parameters. In the parameters table S refers to ‘Seasonal’, IA refers to inter-annual’, ω denotes the period of cosine functions, δ is a scalar factor, Y denotes Young population ($< 20y$) and A Adults (> 20).

Table 1

One population model fitted parameters. Those parameters with no reference were fitted from observed data. Most of the parameters in this table were fitted as described in Section 3.5; those that were not are from bibliographic sources. The parameter P_h was fixed having taken into account the different bibliographic sources (Grunnill, 2018; Vikram et al., 2016; Rafique et al., 2017). As can be seen, for the fitted parameters the 95% confidence interval is shown for each.

No re-susceptibility model				
Parameter	DENV – 3 1989	DENV – 2 1996	DENV – 1 2001	DENV – 1 2006
τ_1 (Andraud et al., 2012)	0.142	0.142	0.142	0.142
τ_2 (Andraud et al., 2012)	0.036	0.036	0.036	0.036
μ (Andraud et al., 2012)	$4.2e - 05$	$4.2e - 05$	$4.2e - 05$	$4.2e - 05$
β_S	0.114 95%CI = [0.112, 0.136]	0.016 95%CI = [0.011, 0.021]	0.014 95%CI = [0.011, 0.016]	0.048 95%CI = [0.042, 0.053]
β_{IA}	0.106 95%CI = [0.098, 0.114]	0.097 95%CI = [0.092, 0.101]	0.047 95%CI = [0.044, 0.049]	0.047 95%CI = [0.042, 0.052]
γ	0.882 95%CI = [0.863, 0.901]	0.552 95%CI [0.527, 0.577]	0.722 95%CI = [0.72, 0.724]	0.592 95%CI = [0.589, 0.595]
P_h	0.4	0.4	0.4	0.4
Re-susceptibility model				
Parameter	DENV – 3 1989	DENV – 2 1996	DENV – 1 2001	DENV – 1 2006
τ_1^r	0.142	0.142	0.142	0.142
τ_2^r	0.036	0.036	0.036	0.036
μ^r	$4.2e - 05$	$4.2e - 05$	$4.2e - 05$	$4.2e - 05$
β_S	0.096 95%CI = [0.0924, 0.0996]	0.023 95%CI = [0.0192, 0.0268]	0.023 95%CI = [0.0192, 0.0268]	0.039 95%CI = [0.0364, 0.0416]
β_{IA}	0.116 95%CI = [0.112, 0.12]	0.665 95%CI = [0.661, 0.669]	0.221 95%CI = [0.217, 0.225]	0.392 95%CI = [0.389, 0.395]
γ	0.609 95%CI = [0.595, 0.623]	0.497 95%CI = [0.494, 0.5]	0.731 95%CI = [0.728, 0.734]	0.732 95%CI = [0.729, 0.735]
P_h	0.4	0.4	0.4	0.4
δ_s	$5.6e - 04$ 95%CI = [4.4e – 4, 2.06e – 3]	$4.2e - 04$ 95%CI = [1.1e – 4, 1.92e – 3]	$2.7e - 01$ 95%CI = [2.5e – 1, 2.8e – 1]	$6.3e - 04$ 95%CI = [1.03e – 4, 2.3e – 3]

Some of the parameters were fixed having taken into account values from published studies, such as τ_i , ϵ and P_h (Grunnill, 2018; Vikram et al., 2016; Rafique et al., 2017)

The fitting algorithm can be summarised as follows:

1. Set the initial set of parameters x using a random uniform distribution with thresholds

2. Set by lb for the lower bound and ub for the upper bound.
3. Run `fmincon` optimisation with the configuration described above.
4. Repeat the previous step until the method achieves convergence
5. Save the resulting parameters in the output set x_0 .
6. Repeat the steps 1–5 until the length of $x_0 = 500$

Table 2

Two population model fitted parameters. Those parameters with no reference were fitted from observed data. As in previous table for one population model, most of the parameters in this table were fitted as described in Section 3.5; those that were not are from bibliographic sources. For the model with re-susceptibility parameter P_h was fixed having taken into account the different bibliographic sources (Grunnill, 2018; Vikram et al., 2016; Rafique et al., 2017). As can be seen, for the fitted parameters the 95% confidence interval is shown for each.

No re-susceptibility model				
Parameter	DENV – 3 1989	DENV – 2 1996	DENV – 1 2001	DENV – 1 2006
τ_1 (Andraud et al., 2012)	0.142	0.142	0.142	0.142
τ_2 (Andraud et al., 2012)	0.036	0.036	0.036	0.036
μ (Andraud et al., 2012)	$4.2e - 05$	$4.2e - 05$	$4.2e - 05$	$4.2e - 05$
β_{SY}	$0.10095\%CI = [0.0931, 0.107]$	$0.12295\%CI = [0.11, 0.13]$	$0.00995\%CI = [6.3e - 2, 0.01]$	$0.01095\%CI = [0.003, 0.017]$
β_{LAY}	$0.06195\%CI = [0.0506, 0.0714]$	$0.05495\%CI = [0.052, 0.055]$	$0.0084595\%CI = [5.9e - 2, 0.01]$	$0.0099795\%CI = [0.003, 0.017]$
γ_Y	$0.60295\%CI = [0.023, 0.101]$	$0.8595\%CI = [0.80, 0.89]$	$0.30195\%CI = [0.29, 0.30]$	$0.48795\%CI = [0.46, 0.51]$
ϵ (Agusto et al., 2017)	$1.4e - 04$	$1.4e - 04$	$1.4e - 04$	$1.4e - 04$
β_{SA}^*	$0.34695\%CI = [0.336, 0.356]$	$0.010495\%CI = [6.7e - 2, 0.014]$	$0.012995\%CI = [0.012, 0.014]$	$0.013795\%CI = [0.007, 0.021]$
β_{LAA}	$0.32195\%CI = [0.31, 0.332]$	$0.01095\%CI = [4.2e - 2, 0.016]$	$0.011895\%CI = [0.008, 0.014]$	$0.058195\%CI = [0.051, 0.065]$
γ_A	$0.61795\%CI = [0.579, 0.655]$	$0.59495\%CI = [0.57, 0.61]$	$0.42395\%CI = [0.42, 0.43]$	$0.55695\%CI = [0.527, 0.585]$
P_h	0.4	0.4	0.4	0.4
Re-susceptibility model				
Parameter	DENV – 3 1989	DENV – 2 1996	DENV – 1 2001	DENV – 1 2006
τ_1 (Andraud et al., 2012)	0.142	0.142	0.142	0.142
τ_2 (Andraud et al., 2012)	0.036	0.036	0.036	0.036
μ (Andraud et al., 2012)	$4.2e - 05$	$4.2e - 05$	$4.2e - 05$	$4.2e - 05$
β_{SY}	$0.30295\%CI = [0.288, 0.316]$	$0.06995\%CI = [0.065, 0.073]$	$0.23395\%CI = [0.218, 0.248]$	$0.24395\%CI = [0.239, 0.247]$
β_{LAY}	$0.06895\%CI = [0.053, 0.082]$	$0.06995\%CI = [0.065, 0.073]$	$0.23695\%CI = [0.221, 0.251]$	$0.04395\%CI = [0.039, 0.046]$
γ_Y	$0.44595\%CI = [0.403, 0.487]$	$0.53695\%CI = [0.518, 0.554]$	$0.73995\%CI = [0.736, 0.742]$	$0.78195\%CI = [0.772, 0.794]$
δ_{Y*}	$0.01595\%CI = [0.011, 0.020]$	$0.00195\%CI = [8.2e - 4, 1.2e - 3]$	$0.03795\%CI = [0.036, 0.038]$	$0.00495\%CI = [0.003, 0.005]$
ϵ (Agusto et al., 2017)	$1.4e - 04$	$1.4e - 04$	$1.4e - 04$	$1.4e - 04$
β_{SA}^*	$0.16295\%CI = [0.147, 0.177]$	$0.06895\%CI = [0.064, 0.072]$	$0.13995\%CI = [0.138, 0.14]$	$0.04695\%CI = [0.043, 0.049]$
β_{LAA}	$0.16495\%CI = [0.148, 0.18]$	$0.06895\%CI = [0.064, 0.072]$	$0.10395\%CI = [0.099, 0.117]$	$0.03595\%CI = [0.032, 0.039]$
γ_A	$0.56495\%CI = [0.522, 0.606]$	$0.52795\%CI = [0.508, 0.546]$	$0.06595\%CI = [0.054, 0.075]$	$0.69495\%CI = [0.686, 0.702]$
δ_{A*}	$1.4e - 0495\%CI = [8.5e - 5, 2e - 4]$	$6.3e - 0495\%CI = [4.9e - 4, 7.7e - 4]$	$0.03195\%CI = [0.030, 0.032]$	$2.5e - 0495\%CI = [1.9e - 4, 3.1e - 4]$
P_h	0.4	0.4	0.4	0.4

Table 3

Error statistics for the different model configurations. \bar{X} is the average, M is the mode, std is the standard deviation, AIC is the Akaike Information Criterion mean value and S is the distribution bias. In this table can be seen how the mean error measure improves significantly when the re-susceptibility parameter is simulated. On the other hand, there is an improved performance when two populations are considered; this can be seen particularly for 2006 wave.

One population no re-susceptibility						
Wave	\bar{X}	M	std	S	Variance	AIC
DENV – 3 1989	$1.45e - 04$	$7.42e - 06$	$1.14e - 04$	$1.23e + 00$	$1.14e - 04$	3.182
DENV – 2 1996	$5.25e - 05$	$6.54e - 07$	$4.88e - 05$	$9.49e - 01$	$4.88e - 05$	2.953
DENV – 1 2001	$6.12e - 06$	0	$8.51e - 06$	$7.54e - 01$	$8.50e - 06$	1.053
DENV – 1 2006	$3.90e - 05$	$4.89e - 07$	$3.07e - 05$	$6.40e - 01$	$3.07e - 05$	2.651
One population with re-susceptibility						
Wave	\bar{X}	M	std	S	Variance	AIC
DENV – 3 1989	$1.34e - 04$	0	$1.12e - 04$	$1.05e - 01$	$1.12e - 04$	2.091
DENV – 2 1996	$5.66e - 05$	$1.41e - 05$	$4.72e - 05$	$6.92e - 01$	$4.72e - 05$	2.713
DENV – 1 2001	$8.48e - 06$	0	$6.88e - 06$	$6.52e - 01$	$6.88e - 06$	0.631
DENV – 1 2006	$4.01e - 05$	$1.40e - 06$	$3.44e - 05$	$3.05e - 01$	$3.44e - 05$	2.201
Two population no re-susceptibility						
Wave	\bar{X}	M	std	S	Variance	AIC
DENV – 3 1989	$1.04e - 04$	0	$1.09e - 04$	$7.35e - 01$	$1.09e - 04$	2.427
DENV – 2 1996	$3.22e - 05$	0	$3.97e - 05$	$6.52e - 01$	$3.97e - 05$	2.494
DENV – 1 2001	$4.68e - 06$	0	$7.37e - 06$	$5.27e - 01$	$7.37e - 06$	0.638
DENV – 1 2006	$3.28e - 05$	0	$2.65e - 05$	$5.56e - 01$	$2.65e - 05$	2.425
Two population with re-susceptibility						
Wave	\bar{X}	M	std	S	Variance	AIC
DENV – 3 1989	$1.32e - 04$	0	$1.02e - 04$	$9.58e - 01$	$1.02e - 04$	2.166
DENV – 2 1996	$3.26e - 05$	0	$2.78e - 05$	$2.24e - 02$	$2.78e - 05$	2.293
DENV – 1 2001	$3.45e - 06$	0	$3.38e - 06$	$5.08e - 01$	$3.38e - 06$	0.608
DENV – 1 2006	$3.57e - 06$	0	$1.23e - 05$	$5.66e - 01$	$1.23e - 05$	2.258

3.6. Model comparison

The different models were numerically validated through the Akaike Information Criterion (AIC); this index provides a measure of model quality considering how well the model can fit the data and at the same time provides a measure of how complex it is. This approach is widely used to measure the quality of models (Symonds and Moussalli,

2011). The AIC index is typically used in modelling as a relative measure of quality in relation to other models, but this measure can be also used to have a metric of accuracy and complexity of the model under consideration (Akaike, 1974, 1976; Samsuzzoha et al., 2013); depending on the value of this index we can infer how good they can support the structural variation of the data. The models that have an AIC index value within the range [1–2] consistently support

Table 4

Errors significance for different model configurations. In the above table we use the Mean Square Error not normalised (\hat{E}), μ is the mean theoretical value, σ is the standard deviation, $\frac{\mu_1 - \mu_2}{\sigma}$ compares the mean theoretical value of each approach with the mean standard deviation and $P(p_1 < p_2)$ is the probability that one of the model's configuration match the data better than the other. The value of P depends on the value of $\frac{\mu_1 - \mu_2}{\sigma}$ as is shown in Table 5.

One population model: re-susceptibility Vs no re-susceptibility					
Model	\hat{E}	μ	σ	$\frac{\mu_1 - \mu_2}{\sigma}$	$P(p_1 < p_2)$
(p_1) Re-susceptibility	15.49	0.992	0.002	0.34	56.92%
(p_2) No re-susceptibility	16.87	0.992	0.002		
Two population model: re-susceptibility Vs no re-susceptibility					
Model	\hat{E}	μ	σ	$\frac{\mu_1 - \mu_2}{\sigma}$	$P(p_1 < p_2)$
(p_1) Re-susceptibility	11.54	0.994	0.0018	0.35	56.92%
(p_2) No re-susceptibility	12.98	0.994	0.0018		
Two population model Vs one population model: No re-susceptibility					
Model	\hat{E}	μ	σ	$\frac{\mu_1 - \mu_2}{\sigma}$	$P(p_1 < p_2)$
(p_1) Two population	12.98	0.992	0.002	1.01	80.78%
(p_2) One populations	16.87	0.994	0.0018		
Two population model Vs one population model: Re-susceptibility					
Model	\hat{E}	μ	σ	$\frac{\mu_1 - \mu_2}{\sigma}$	$P(p_1 < p_2)$
(p_1) Two population	11.54	0.992	0.0020	1.08	80.8%
(p_2) One populations	15.49	0.994	0.0017		
One population model (no re-susceptibility) Vs two population model (re-susceptibility)					
Model	\hat{E}	μ	σ	$\frac{\mu_1 - \mu_2}{\sigma}$	$P(p_1 < p_2)$
(p_1) Two population	11.54	0.992	0.0020	1.43	80.81
(p_2) One populations	16.87	0.994	0.0017		

Table 5

Relation for the Hypothesis test described in Section 3.6.

$\frac{\mu_1 - \mu_2}{\sigma}$	$P(p_1 < p_2)$
0.0	50.00
0.5	63.81
1.0	76.02
1.5	85.54
2.0	92.13
2.5	96.16
3.0	98.30
3.5	99.33
4.0	99.77
4.5	99.93
5.0	99.98
5.5	99.99

structural variation in the data. The models that have their value in the range [3–7] withstand significantly structural variation in the data. Finally, those models that have their AIC index > 10 do not explain any important structural changes in the data (Fang, 2011; Posada and Buckley, 2004). The index is calculated according to Eq. (5)

$$AIC = \log(\det(\frac{1}{m} \sum_1^m \epsilon(t, \theta)(\epsilon(t, \theta))^T)) + \frac{2n}{m} \tag{5}$$

where θ is the set of n estimated parameters m is the number of samples and $\epsilon(t, \theta)$ is the measure of error. The measure of error here used was the normalised residuals. The reason for choosing this method and not a Bayesian method, such as the Bayesian Information Criterion (BIC), is because the index obtained by AIC is an estimate of a constant plus relative distance between the true unknown function and the model function, so a lower AIC represents a model closer to the reality.

The S bias is calculated through the second Pearson coefficient of the form $S = 3(\bar{X} - Md)/std$, where Md is the median. The bias coefficient gives an idea of the skews of the distribution, if $S > 0$ the skews of the distribution is positive, if $S < 0$ the skew is negative and if $S = 0$ the distribution is symmetric. This means that the closer to 0 the value of S is, the better the approximation of the model. Results are summarised in Table 3

To compare the different configurations of the model, we also estimate the probability of error for each possible configuration, comparing them with each other to determine which of the possible configurations best fits the data. In this case, the error measure we use for the analysis was $\hat{E} = \sqrt{\sum_{i=1}^N (I_i^{model} - I_i^{observed})^2}$, to have a measure unaffected by normalisation. To perform this hypothesis test we assume the statistical independence of the fitting errors for different data sets and we approach the errors of a binomial distribution by a Gaussian distribution (Highleyman, 1962; López et al., 2020). This is possible because we have a high enough number of records for each experiment, this means the total number experiments is $n = 2000$ (500 experiments for each epidemic wave). For each model configuration having into account all the DENV epidemic waves we test hypothesis $P(\hat{E}_{m_1} < \hat{E}_{m_2}) > p$, where m_1 and m_2 were the two different configurations. In Table 4 the results of the test are summarised, here the mean $\mu = 1 - (\hat{E}/n)$ and the standard deviation is $\sigma = \sqrt{\mu(1 - \mu)/n}$. The significance of the test is established in Table 5, to establish these relationships we use a binomial error model for what was explained above.

4. Results

The age-incidence profiles were studied for six of the epidemics during the study period: DENV-1 1988, DENV-3 1989, DENV-2 1996, DENV-1 2001, DENV-1 2006 and DENV-4 2009. The first DENV-4 1979 was not analysed as the data set was incomplete and the 2013/14 epidemic was multitypic and thus also not analysed. The incidence rates, per 10,000 individuals, ranged from 120–290 for suspected cases and from 30–90 for laboratory confirmed cases. The vast majority of cases occurred on the principal and most populated island of Tahiti during any of the epidemics. Age stratification according to potential exposure to previous epidemics of the same serotype revealed clear evidence of age-specific protection, with significantly reduced relative risk of disease in individuals of an age at which they could have been previously exposed (Fig. 2). A notable exception was the young age group (5–14 years) in 2006, old enough to have been exposed in the 2001 DENV-1 epidemic, but who had the same risk as the naïve children under 5 years of age (Fig. 2).

Age stratification according to potential previous exposure to a heterotypic serotype revealed significantly increased risk of disease

in individuals with previous heterotypic exposure, consistent with the paradigm of increased disease risk in secondary infections. The notable exception was the DENV-3 1989 epidemic that occurred back-to-back with the DENV-1 1988 epidemic, where individuals of an age to have had a secondary infection did not have increased risk of clinical disease (Fig. 2). This latter result is consistent with short-term cross-protective immunity, suggested to last 8–18 months (Sabin et al., 1952; Salje et al., 2012; Reich et al., 2013). Thus, globally, the age incidence profiles were consistent with classical paradigms of protection and enhancement, despite a relatively small number of reported clinical cases. Increased risk of clinical disease with a heterotypic infection seemingly occurred predominantly only in the case of a first heterotypic infection and not subsequent ones, although the outcomes are quite variable. The striking age-specific patterns of reduced homotypic and increased heterotypic clinical risk, despite the low reported incidence rates, would suggest a considerable number of unreported, sub-clinical infections had occurred.

To explore the roles of asymptomatic infections and waning homotypic immunity, we developed dynamical models incorporating several new features: (i) a novel infected group, “asymptomatic infections”, (ii) the potential for an infected individual to become susceptible once again to the same serotype and (iii) age structure, for which an age cut-off of 20 years of age was chosen, being the average time interval between homotypic epidemics (Fig. 3). These novel parameterised models were then applied to four of the epidemics: the DENV-3 1989, the DENV-2 1996 epidemic and the twin DENV-1 2001/6 epidemics. Globally, inclusion of age structure and re-susceptibility parameters improved the goodness of fit of the models for all four epidemics, capturing the temporality and amplitude of the epidemic waves with increasing accuracy (Fig. 4). This also can be seen in Table 3 by checking on the column of mean error (\bar{X}). As can be seen, those models in which the population was split into two different groups and the re-susceptibility parameter is included are much better than for the more simpler configurations; this is particularly true for the waves of 1996, 2001 and 2006. We also can see this graphically in Fig. 6 in which the variance of the error is plotted, suggesting these more ‘complex’ configurations give stability to the model’s output. This was borne out by improving Akaike Information Criterion (AIC) values when age structure and re-susceptibility were included (Fig. 4). The relative influence of these two added features, however, altered considerably according to the epidemic (Tables 1 & 2). Of particular note was that the re-susceptibility parameter for the DENV-1 2001 epidemic is 100–1000 times higher than any of the other epidemics, even the DENV-1 2006 epidemic. Inclusion of age structure improved the model fit for the DENV-2 and DENV-3 epidemics, and less so for the DENV-1 epidemics. This may reflect the fact that the previous DENV-2 and DENV-3 epidemics had occurred approximately 20 years prior to the current homotypic epidemics (24 and 25 years respectively), thus mirroring more closely the age structure used in the model. The estimated transmission rate in the younger population was indeed found to be near to 10 times higher than in the older population in the DENV-2 epidemic, consistent with the acquisition of previous immunity in the older population. This can be seen in the values of the force of infection (Table 2).

The estimated percentage of DENV infections that were asymptomatic was high during all epidemics, ranging from 66–90% and was highest in the DENV-1 paired epidemics (Fig. 5). Such a high percentage of asymptomatic infections is consistent with serological surveys performed in this population and the age incidence risk profiles observed here, despite relatively few clinical infections reported during any single epidemic (Aubry et al., 2018). The asymptomatic percentage varied little (< 10% variation) across models for the DENV-2 and DENV-3 epidemics, but ~ 20% for the DENV-1 epidemics, with most significant variation occurring when the re-susceptibility parameter was included. This could suggest that the proposed waning immunity, implicit in the re-susceptibility parameter, led to increased likelihood

of a symptomatic infection outcome despite following a previously homotypic infection.

Table 3 shows the model’s results support our hypothesis of re-susceptibility clearly. This can be seen particularly for some waves such as DENV-1 2001 and 2006. On the other hand, in general terms, all of the model’s configurations support data variation. As can be seen in Table 3, for most of the epidemic waves under study, both the mean error and standard deviation (but also the variance) are significantly lower for the model incorporating the re-susceptibility parameter and these results further improve when two populations are considered (Fig. 6). Table 4 shows the results of the statistical robustness test that was carried out as explained in Section 3.6. In it you can see the different configurations of the model that were compared with each other to establish which configuration is better than the other. To calculate the error of the models, all DENV epidemics were taken into account. In this sense, it can be said that when talking about the model for a population without re-susceptibility, the adjustment error of said model for the 1989 DENV-3, 1996 DENV-2, 2001 DENV-1 and 2006 DENV-1 waves is taken into account, and the same for all the configurations. As can be seen, the table is divided into 5 sub-tables where each one represents the results for each performed test. The possible configurations we compared are: one population model (with re-susceptibility parameter Vs no re-susceptibility parameter), two population model (with re-susceptibility parameter Vs no re-susceptibility parameter), two population model Vs one population model (with re-susceptibility parameter) and one population model (without re-susceptibility parameter) Vs two population model (with re-susceptibility parameter). In Table 5 the values of P for each interval is shown.

5. Discussion

Waning of antibodies and time since previous dengue heterotypic infection have been highlighted as being influential in determining whether a new heterotypic infection will result in a cross-protective or enhancing outcome (Katzelnick et al., 2016; Salje et al., 2018). It now seems that such waning immunity can also impact on immunity to homotypic infections and, as suggested for Zika, renders individuals re-susceptible (Henderson et al., 2020). As observed before, there is variation in viral genotypic virulence and transmissibility and thus, as suggested by the DENV-1 2001 Pacific genotype, likely variation in immunogenicity (Steel et al., 2010). The very high re-susceptibility rates estimated for the 2001 DENV-1 epidemic suggest induction of a poor or short-lasting immune response and provide some explanation for the hyper-endemic circulation of that serotype in French Polynesia. In addition, phylogenetic analysis of this genotype revealed that the virus underwent significant genetic diversification from 2002, which could also explain its re-emergence in 2006, the lack of reduced relative risk in children potentially exposed in 2001 and the different best fit model parameter values for what was considered as the same viral genotype (Descloux et al., 2009). In 2013, only four years after the DENV-1 Pacific genotype IV had completely disappeared, the Asian genotype I emerged and DENV-1 recirculated for six years (Aubry et al., 2018). This would suggest that the Pacific genotype elicits a poor level of persistent immunity. The extent to which such waning or imperfect immunity is a feature of DENV-1, or indeed all serotypes, remains to be elucidated but improved model fits for all the epidemics here suggest it might be. Indeed, a previous study on DENV-2 found waning levels of neutralising antibodies that afforded incomplete protection against homotypic infection and disease (Kosasih et al., 2016). Overall, this begs the question of how within genotype evolution can lead to evasion of previously acquired immunity to the same serotype.

The vast majority of infections were estimated to be asymptomatic (Fig. 5), in line with previous studies (Grange et al., 2014). In the dynamical models, the recovery and re-susceptibility rate parameters

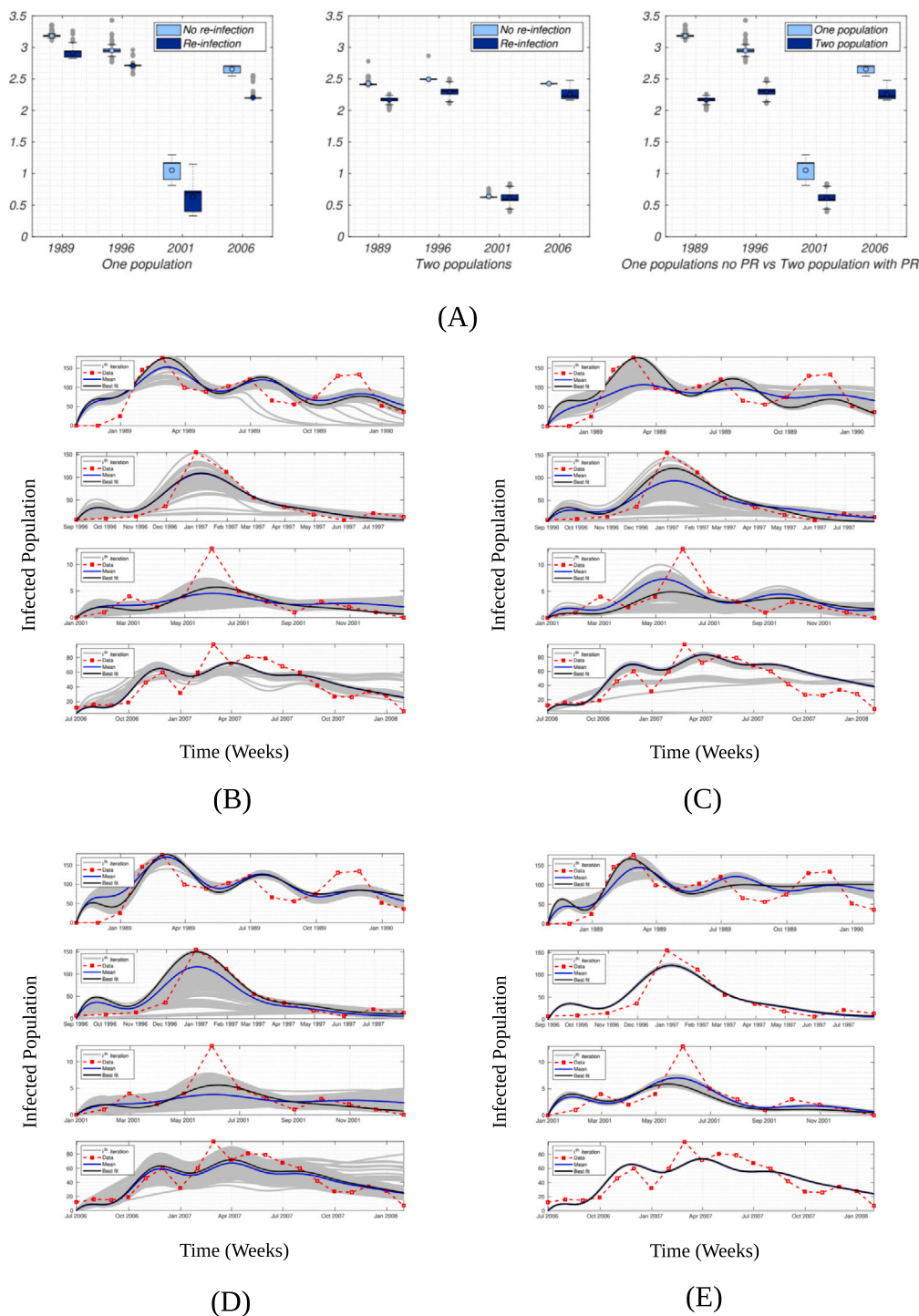


Fig. 4. Fitting and validation of the different models. (A) Comparison of AIC indices for the model with one population (left), two populations (centre), and one population vs two populations (right). (B) Model of a single population, without re-susceptibility by the same serotype. (C) Model of a single population, with re-susceptibility by the same serotype. (D) Model of two populations, without re-susceptibility by the same serotype. (E) Model of two populations, with re-susceptibility by the same serotype. The number of simulations performed in each case is 500. A particularly interesting result can be seen in the lower dispersion in the predictions for the model with two populations and re-susceptibility.

were shared by both the symptomatic and asymptomatic classes. Insofar as such asymptomatic infections are infectious to mosquitoes (Duong et al., 2015) and driving the epidemic through their predominance, it would seem reasonable to assume that model parameters are those generated by the asymptomatic class. With the exception of the DENV-1 2001 epidemic, parameter values for the re-susceptibility rate were very small, therefore suggesting that for the most part asymptomatic

infections are generating homotypic immunity and the subsequent age-risk profiles observed in the epidemiological analyses.

The incorporation of a re-susceptibility parameter (δ_i^*) in the population model clearly improves the predictive capacity of the model. This can be seen in Table 3, where different statistical measures of the models are summarised for each of the configurations, but also, more generally, in Table 4 (these being complementary to the results of Table 3), where the test carried out shows that the best approximation

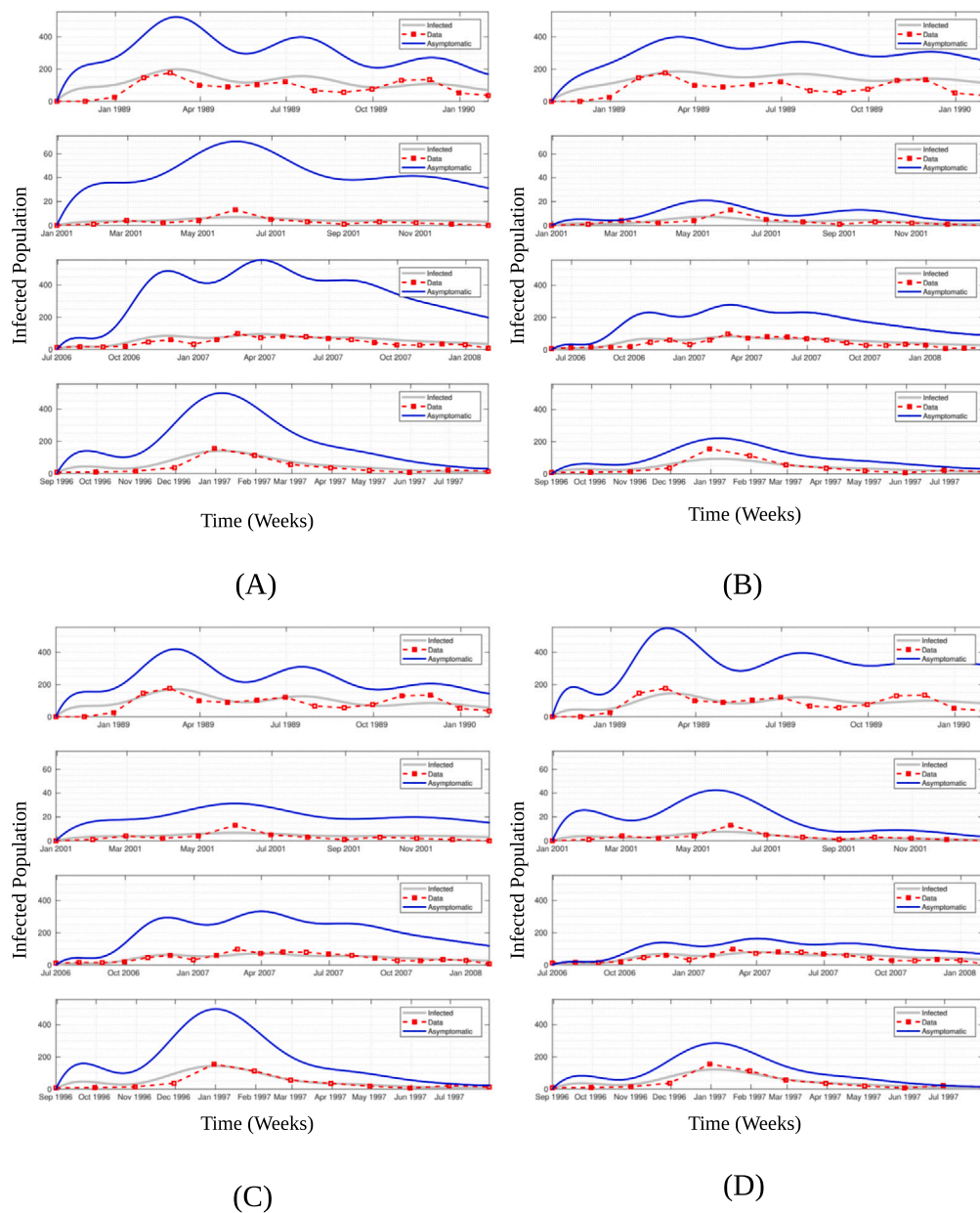


Fig. 5. Asymptomatic mean dynamics Vs symptomatic mean dynamics of the different models. (A) Model of a single population, without re-susceptibility by the same serotype. (B) Model of a single population, with re-susceptibility by the same serotype. (C) Model of two populations, without re-susceptibility by the same serotype. (D) Model of two populations, with re-susceptibility by the same serotype. Each figure represents the mean asymptomatic dynamics of the 500 iterations against the symptomatic population's dynamics. It is important to see that in this figure only the mean behaviour of the model is shown for both symptomatic and asymptomatic populations dynamics.

is the one that includes the separation of the population into age groups and incorporates the loss of immunity.

More broadly, our work suggests that incorporating relatively simple additions to classical *SEIR* models can yield significant improvements to modelling epidemiological profiles. In particular, the inclusion of asymptomatic and re-susceptibility parameters can reveal fundamental immunological characteristics of responses to infection. They may offer a robust alternative to characterising the broad dengue epidemiological picture when serological data are lacking, and whenever available data do not provide clear information on protection and sensitivity to viral variation.

This study has several limitations. First, it is based on clinically reported cases and therefore subject to under-reporting, which may differ geographically. Despite geographical heterogeneity in both DENV transmission and under-reporting, the age-structured patterns in homotypic protection and heterotypic susceptibility are very evident. This

would suggest that DENV exposure is relatively homogeneous, at least on the major island of Tahiti where most of the population reside and cases occurred. Second, the dynamical model simulations were only performed for this major island and did not take into account flux of DENV among all the sub-divisions. Implementation of a meta-population approach could alter the conclusions reached, although the vast majority of cases occurred on this major island and it is likely the source of DENV for the whole of French Polynesia. Thirdly, not all cases were serotyped. We previously defined an epidemic period using a threshold method and then assumed all cases were of the serotype causing the epidemic. It is likely that the serotype of some of the cases were misassigned, especially during the early stages of the epidemic.

In conclusion, dengue is still a major public health problem in tropical areas and is projected to become a significant risk in temperate countries where mosquito vectors are gaining geographical expansion (Liu-Helmersson et al., 2019; Colón-González et al., 2021). The

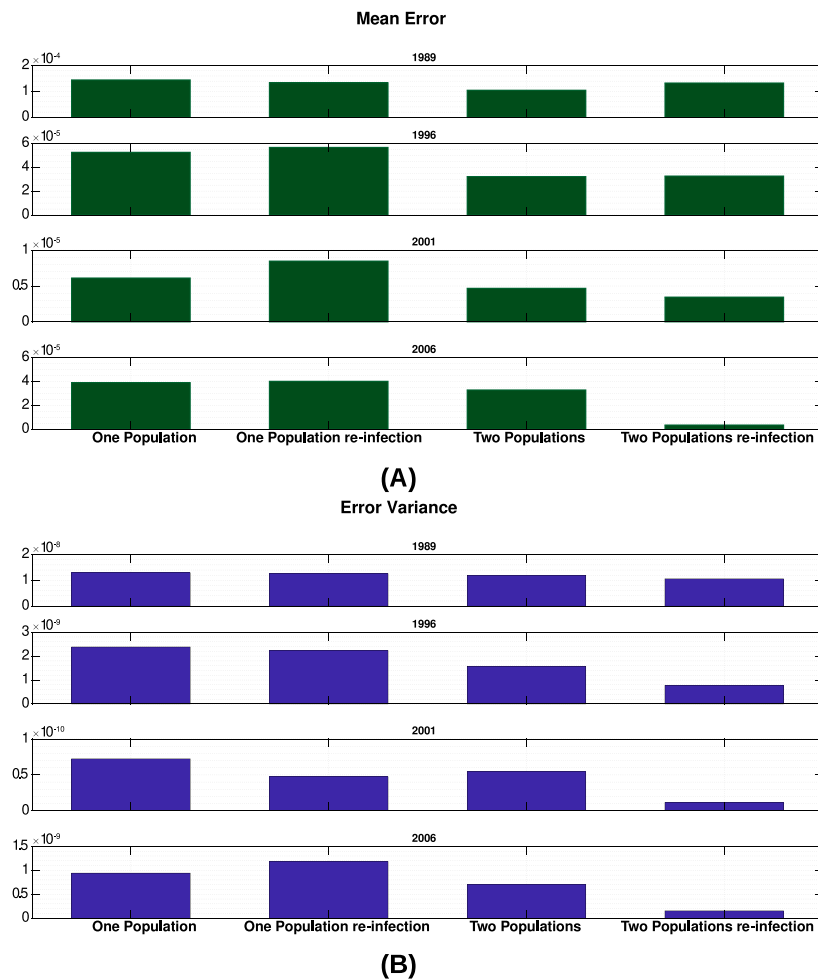


Fig. 6. Error measures for the different models configurations. (A) Mean model Error (B) Error's variance, with re-susceptibility by the same serotype. These measures were calculated by taking into account the full set of 500 simulations.

development of a dengue vaccine able to provide full protection against risk of severe clinical illness still remains the desired solution to significantly reduce the burden of the disease. However, current implemented or trialled vaccines are only partly effective (Capeding et al., 2014; da Silveira et al., 2019). Our study shows that immunity to DENV can be imperfect and potentially even wane over time. Even partially effective vaccines, if against all 4 serotypes, may be of public health value, as they could prevent immunity waning and confer protection against severe disease in at-risk previously exposed age groups. In our COVID-19 redesigned world, where partially effective vaccines are promoted to everybody to protect at-risk individuals (the elderly or people with co-morbidities), particularly because the perspective of getting at-risk groups 100 percent vaccinated becomes increasingly difficult, using similar strategies to combat dengue should be considered.

CRedit authorship contribution statement

Leonardo López: Conceived the study, Formulated the epidemiological model, Wrote the paper, Conducted parameter estimation, Implemented the different model configurations, Ran the simulations, Final writing and discussion. **Richard E. Paul:** Conceived the study, Formulated the epidemiological model and wrote the paper, Final writing and discussion. **Van-Mai Cao-Lormeau:** Provided the dengue historical time series, Final writing and discussion. **Xavier Rodó:** Conceived the study, Formulated the epidemiological model and wrote the paper, Provided epidemiological expertise, Participated in the mathematical modelling, Final writing and discussion.

Declaration of competing interest

The authors declare that they have no known competing financial interests or personal relationships that could have appeared to influence the work reported in this paper.

Data and materials availability

The data are fully available and can be accessed via this link. <https://figshare.com/s/deebd75b84e742c1803f>

Acknowledgements

XR and LL acknowledge support from the Spanish Ministry of Science and Innovation through the 'Centro de Excelencia Severo Ochoa 2019 2023' Program (CEX2018 000806S), and support from the Generalitat de Catalunya through the CERCA Program.

Funding

The research leading to these results has received funding from the European Commission Seventh Framework Program [FP7/2007–2013] for the DENFREE project under Grant Agreement n282378 to RP, XR, VMCL. The funders had no role in study design, data collection and analysis, decision to publish or preparation of the manuscript.

References

- Agusto, F.B., Bewick, S., Fagan, W., 2017. Mathematical model of Zika virus with vertical transmission. *Infect. Dis. Model.* 2 (2), 244–267.
- Akaike, H., 1974. A new look at the statistical model identification. *IEEE Trans. Automat. Control* 19 (6), 716–723.
- Akaike, H., 1976. An information criterion (AIC). *Math. Sci.* 14, 5–7.
- Andraud, M., Hens, N., Marais, C., Beutels, P., 2012. Dynamic epidemiological models for dengue transmission: a systematic review of structural approaches. *PLoS One* 7 (11), e49085.
- Aubry, M., Cao-Lormeau, V.-M., 2019. History of arthropod-borne virus infections in French Polynesia. *New Microbes New Infect.* 29, 100513.
- Aubry, M., Teissier, A., Huart, M., Merceron, S., Vanhomwegen, J., Mapotoe, M., Mariteragi-Helle, T., Roche, C., Vial, A.-L., Teururai, S., et al., 2018. Seroprevalence of dengue and chikungunya virus antibodies, French Polynesia, 2014–2015. *Emerg. Infect. Diseases* 24 (3), 558.
- Capeding, M.R., Tran, N.H., Hadinegoro, S.R.S., Ismail, H.I.H.M., Chotpitayanusondh, T., Chua, M.N., Luong, C.Q., Rusmil, K., Wirawan, D.N., Nallusamy, R., et al., 2014. Clinical efficacy and safety of a novel tetravalent dengue vaccine in healthy children in Asia: a phase 3, randomised, observer-masked, placebo-controlled trial. *Lancet* 384 (9951), 1358–1365.
- Colón-González, F.J., Sewe, M.O., Tompkins, A.M., Sjödin, H., Casallas, A., Rocklöv, J., Caminade, C., Lowe, R., 2021. Projecting the risk of mosquito-borne diseases in a warmer and more populated world: a multi-model, multi-scenario intercomparison modelling study. *Lancet Planet. Health* 5 (7), e404–e414.
- da Silveira, L.T.C., Tura, B., Santos, M., 2019. Systematic review of dengue vaccine efficacy. *BMC Infect. Dis.* 19 (1), 1–8.
- Descoux, E., Cao-Lormeau, V.-M., Roche, C., De Lamballerie, X., 2009. Dengue 1 diversity and microevolution, French Polynesia 2001–2006: connection with epidemiology and clinics. *PLoS Negl. Trop. Dis.* 3 (8), e493.
- Duong, V., Lambrechts, L., Paul, R.E., Ly, S., Lay, R.S., Long, K.C., Huy, R., Taranatola, A., Scott, T.W., Sakuntabhai, A., et al., 2015. Asymptomatic humans transmit dengue virus to mosquitoes. *Proc. Natl. Acad. Sci.* 112 (47), 14688–14693.
- Endy, T.P., Nisalak, A., Chunsuttiwat, S., Vaughn, D.W., Green, S., Ennis, F.A., Rothman, A.L., Libraty, D.H., 2004. Relationship of preexisting dengue virus (DV) neutralizing antibody levels to viremia and severity of disease in a prospective cohort study of DV infection in Thailand. *J. Infect. Dis.* 189 (6), 990–1000.
- Fang, Y., 2011. Asymptotic equivalence between cross-validations and Akaike information criteria in mixed-effects models. *J. Data Sci.* 9 (1), 15–21.
- Gallichotte, E.N., Baric, T.J., Nivarthi, U., Delacruz, M.J., Graham, R., Widman, D.G., Yount, B.L., Durbin, A.P., Whitehead, S.S., de Silva, A.M., et al., 2018. Genetic variation between dengue virus type 4 strains impacts human antibody binding and neutralization. *Cell Rep.* 25 (5), 1214–1224.
- Grange, L., Simon-Loriere, E., Sakuntabhai, A., Gresh, L., Paul, R., Harris, E., 2014. Epidemiological risk factors associated with high global frequency of inapparent dengue virus infections. *Front. Immunol.* 5, 280.
- Grunnill, M., 2018. An exploration of the role of asymptomatic infections in the epidemiology of dengue viruses through susceptible, asymptomatic, infected and recovered (SAIR) models. *J. Theoret. Biol.* 439, 195–204.
- Halstead, S.B., Katzelnick, L.C., Russell, P.K., Markoff, L., Aguiar, M., Dans, L.R., Dans, A.L., 2020. Ethics of a partially effective dengue vaccine: Lessons from the Philippines. *Vaccine* 38 (35), 5572–5576.
- Halstead, S.B., et al., 2003. Neutralization and antibody-dependent enhancement of dengue viruses. *Adv. Virus Res.* 60, 421–467.
- Henderson, A.D., Aubry, M., Kama, M., Vanhomwegen, J., Teissier, A., Mariteragi-Helle, T., Paoaafaita, T., Teissier, Y., Manuguerra, J.-C., Edmunds, J., et al., 2020. Zika seroprevalence declines and neutralizing antibodies wane in adults following outbreaks in French Polynesia and Fiji. *Elife* 9, e48460.
- Highleyman, W.H., 1962. The design and analysis of pattern recognition experiments. *Bell Syst. Tech. J.* 41 (2), 723–744.
- ISPF, 2018. ISPF. Population légale - ISPF. <https://www.ispf.org/bases/Recensements/2017/poplegale.aspx%202017>. (Accessed 16 November 2018).
- Katzelnick, L.C., Fonville, J.M., Gromowski, G.D., Arriaga, J.B., Green, A., James, S.L., Lau, L., Montoya, M., Wang, C., VanBlargan, L.A., et al., 2015. Dengue viruses cluster antigenically but not as discrete serotypes. *Science* 349 (6254), 1338–1343.
- Katzelnick, L.C., Harris, E., Baric, R., Collier, B.-A., Coloma, J., Crowe Jr., J.E., Cummings, D.A., Dean, H., de Silva, A., Diamond, M.S., et al., 2017. Immune correlates of protection for dengue: state of the art and research agenda. *Vaccine* 35 (36), 4659–4669.
- Katzelnick, L.C., Montoya, M., Gresh, L., Balmaseda, A., Harris, E., 2016. Neutralizing antibody titers against dengue virus correlate with protection from symptomatic infection in a longitudinal cohort. *Proc. Natl. Acad. Sci.* 113 (3), 728–733.
- Kosasih, H., Alisjahbana, B., de Mast, Q., Rudiman, I.F., Widjaja, S., Antonjaya, U., Novriani, H., Susanto, N.H., Jusuf, H., van der Ven, A., et al., 2016. The epidemiology, virology and clinical findings of dengue virus infections in a cohort of Indonesian adults in Western Java. *PLoS Negl. Trop. Dis.* 10 (2), e0004390.
- Liu-Helmersson, J., Rocklöv, J., Sewe, M., Brännström, A., 2019. Climate change may enable *Aedes Aegypti* infestation in major European cities by 2100. *Environ. Res.* 172, 693–699.
- López, L., Fernandez, M., Gómez, A., Giovanini, L., 2020. An influenza epidemic model with dynamic social networks of agents with individual behaviour. *Ecol. Complex.* 41, 100810.
- Payne, R.W., 2009. *GenStat*. Wiley Interdiscip. Rev. Comput. Stat. 1 (2), 255–258.
- Posada, D., Buckley, T.R., 2004. Model selection and model averaging in phylogenetics: advantages of Akaike information criterion and Bayesian approaches over likelihood ratio tests. *Syst. Biol.* 53 (5), 793–808.
- Rafique, I., Saqib, M.A.N., Munir, M.A., Qureshi, H., Iqbal, R., Ahmed, W., Akhtar, T., et al., 2017. Asymptomatic dengue infection in adults of major cities of Pakistan. *Asian Pacific J. Trop. Med.* 10 (10), 1002–1006.
- Reich, N.G., Shrestha, S., King, A.A., Rohani, P., Lessler, J., Kalayanarooj, S., Yoon, I.-K., Gibbons, R.V., Burke, D.S., Cummings, D.A., 2013. Interactions between serotypes of dengue highlight epidemiological impact of cross-immunity. *J. R. Soc. Interface* 10 (86), 20130414.
- Sabin, A.B., et al., 1952. Research on dengue during world war II. *Am. J. Trop. Med. Hyg.* 1 (1), 30–50.
- Salje, H., Cummings, D.A., Rodriguez-Barraquer, I., Katzelnick, L.C., Lessler, J., Klungthong, C., Thaisomboonsuk, B., Nisalak, A., Weg, A., Ellison, D., et al., 2018. Reconstruction of antibody dynamics and infection histories to evaluate dengue risk. *Nature* 557 (7707), 719–723.
- Salje, H., Lessler, J., Endy, T.P., Curriero, F.C., Gibbons, R.V., Nisalak, A., Nimmannitya, S., Kalayanarooj, S., Jarman, R.G., Thomas, S.J., et al., 2012. Revealing the microscale spatial signature of dengue transmission and immunity in an urban population. *Proc. Natl. Acad. Sci.* 109 (24), 9535–9538.
- Salje, H., Rodriguez-Barraquer, I., Rainwater-Lovett, K., Nisalak, A., Thaisomboonsuk, B., Thomas, S.J., Fernandez, S., Jarman, R.G., Yoon, I.-K., Cummings, D.A., 2014. Variability in dengue titer estimates from plaque reduction neutralization tests poses a challenge to epidemiological studies and vaccine development. *PLoS Negl. Trop. Dis.* 8 (6), e2952.
- Samsuzzoha, M., Singh, M., Lucy, D., 2013. Parameter estimation of influenza epidemic model. *Appl. Math. Comput.* 220, 616–629.
- Steel, A., Gubler, D.J., Bennett, S.N., 2010. Natural attenuation of dengue virus type-2 after a series of island outbreaks: a retrospective phylogenetic study of events in the South Pacific three decades ago. *Virology* 405 (2), 505–512.
- Symonds, M.R., Moussalli, A., 2011. A brief guide to model selection, multimodel inference and model averaging in behavioural ecology using Akaike's information criterion. *Behav. Ecol. Sociobiol.* 65 (1), 13–21.
- Teissier, Y., Paul, R., Aubry, M., Rodo, X., Dommar, C., Salje, H., Sakuntabhai, A., Cazelles, B., Cao-Lormeau, V.-M., 2020. Long-term persistence of monotypic dengue transmission in small size isolated populations, french polynesia, 1978–2014. *PLoS Negl. Trop. Dis.* 14 (3), e0008110.
- Vikram, K., Nagpal, B., Pande, V., Srivastava, A., Saxena, R., Anvikar, A., Das, A., Singh, H., Gupta, S.K., Tuli, N., et al., 2016. An epidemiological study of dengue in Delhi, India. *Acta Tropica* 153, 21–27.
- Waggoner, J.J., Balmaseda, A., Gresh, L., Sahoo, M.K., Montoya, M., Wang, C., Abeynayake, J., Kuan, G., Pinsky, B.A., Harris, E., 2016. Homotypic dengue virus reinfections in Nicaraguan children. *J. Infect. Dis.* 214 (7), 986–993.
- Waggoner, J.J., Gresh, L., Mohamed-Hadley, A., Balmaseda, A., Soda, K.J., Abeynayake, J., Sahoo, M.K., Liu, Y., Kuan, G., Harris, E., et al., 2017. Characterization of dengue virus infections among febrile children clinically diagnosed with a non-dengue illness, Managua, Nicaragua. *J. Infect. Dis.* 215 (12), 1816–1823.
- Yeo, A.S., Azhar, N.A., Yeow, W., Talbot Jr., C.C., Khan, M.A., Shankar, E.M., Rathakrishnan, A., Azizan, A., Wang, S.M., Lee, S.K., et al., 2014. Lack of clinical manifestations in asymptomatic dengue infection is attributed to broad down-regulation and selective up-regulation of host defence response genes. *PLoS One* 9 (4), e92240.